The C-Terminus of Troponin T Is Essential for Maintaining the Inactive State of Regulated Actin

Andrew J. Franklin,[†] Tamatha Baxley,[†] Tomoyoshi Kobayashi,[‡] and Joseph M. Chalovich[†*]
[†]Department of Biochemistry and Molecular Biology, Brody School of Medicine, East Carolina University, Greenville, North Carolina; and
[‡]Department of Physiology and Biophysics and Center for Cardiovascular Research, College of Medicine, University of Illinois, Chicago, Illinois

ABSTRACT Striated muscle contraction is regulated by the actin binding proteins tropomyosin and troponin. Defects in these proteins lead to myopathies and cardiomyopathies. Deletion of the 14 C-terminal residues of cardiac troponin T leads to hypertrophic cardiomyopathy. We showed earlier that regulated actin containing Δ14 TnT was more readily activated than wild-type regulated actin. We suggested that the equilibria among the inactive (blocked), intermediate (closed or calcium), and active (open or myosin) states was shifted to the active state. We now show that, in addition, such regulated actin filaments cannot enter the inactive or blocked state. Regulated actin containing Δ14 TnT had ATPase activities in the absence of Ca^{2+} that were higher than wild-type filaments but far below the fully active rate. The rapid dissociation of S1-ATP from regulated actin filaments containing Δ14 TnT and acrylodan-labeled tropomyosin did not show the fluorescence increase characteristic of moving to the inactive state. Replacing wild-type TnI with S45E TnI, that favors the inactive state, did not restore the fluorescence change. We conclude that TnT has a previously unrecognized role in forming the inactive state of regulated actin.

INTRODUCTION

Cardiac and skeletal muscles are regulated by the actin binding proteins tropomyosin, troponin I, troponin T, and troponin C. The complex of actin, tropomyosin, and the three troponin components leads to regulated actin with varied abilities to stimulate the ATPase activity of myosin. The presence of high-affinity interactions with myosin stabilizes the active state. Saturating Ca^{2+} favors the formation of the intermediate state. In the absence of high-affinity myosin interactions or Ca^{2+}, the regulated actin is inactive.

Alterations in troponin, such as disease-causing mutations, may lead to changes in distribution of states of the regulatory complex (1–3), resulting in ATPase rates that are too high or too low. If the distribution of states could be normalized it might be possible to avoid the progression to heart failure. Molecular dynamics simulations (4) and experimental results (5,6) show close coupling of the components of the troponin complex. This close coupling raises the possibility that an abnormal distribution of states might be corrected by perturbing troponin at a site distant from initial mutation. However, before such an approach is to be taken, it is necessary to understand more clearly the role of the TnT, TnI, and TnC subunits of troponin.

The TnT subunit of troponin is sometimes thought of as a glue that holds TnI and TnC to tropomyosin (7). TnT is thought to be involved in obtaining full activation of contraction but is not considered to play a key role in the inactivation process. Our work shows that TnT may play an essential role in maintaining the inactive state of regulated actin.

Deletion of the 14 C-terminal residues of TnT resulted in higher actin-activated ATPase activity in the presence and absence of Ca^{2+} relative to wild-type when normalized to the maximum possible activation obtained in the presence of the activator NEM-S1 (3). Those results were interpreted as stabilization of the active state of regulated actin by Δ14 TnT (3).

We now show from an analysis of ATPase activities and from changes in acrylodan-tropomyosin fluorescence that deletion of those 14 residues of TnT also restricted entry of regulated actin into the inactive state. That restriction was severe and could not be rescued by a TnI mutant (S45E) that favors the inactive state (3). The S45E mutation of TnI mimics protein kinase C phosphorylation of TnI (2).

METHODS

Proteins

Actin (8) and skeletal muscle troponin (9) were prepared from rabbit back muscle. Myosin was prepared either from rabbit back muscle (10) or porcine left ventricle (11,12). Myosin S1 was prepared by chymotryptic digestion of myosin (12,13). Cardiac S1 was further purified by cosedimentation with equimolar actin at 0.3 M KCl buffer and 1 mM MgATP (14). Cardiac muscle tropomyosin (15) and troponin (16) were prepared from bovine cardiac left ventricles. Human cardiac troponin TnT (isoform 2) in pSBETa, TnC in pET3d, human cardiac TnI in pET17b, and mouse cardiac TnI in pET3d were expressed and purified as previously described (3,17).

Troponin subunits were reconstituted following the previously described protocol (17) with some modifications. TnT, TnI, and TnC were mixed at a 1:1:1.2 molar ratio and a Protein Pak DEAE 15HR column (Waters, Milford, MA) was used for final purification with start buffer of 0.1 M NaCl, 20 mM Tris-HCl pH 8.0, and 5 mM $MgCl_2$. Troponin was eluted with a 0.1–1.0 M NaCl gradient in the same buffer. The troponin used was either all human cardiac or else a hybrid formed from human cardiac TnT and TnC and mouse cardiac TnI. The latter combination allowed us to use a phosphomimetic mutant of that TnI that stabilized the inactive state.

Protein concentrations were determined using the following extinction coefficients: ($\varepsilon^{0.1\%}$) for 280-nm: actin, 1.15 and myosin S1, 0.75. Concentrations of tropomyosin and troponin subunits were determined with

Submitted November 8, 2011, and accepted for publication April 24, 2012.
*Correspondence: chalovichj@ecu.edu
Editor: James Sellers.

0006-3495/12/06/2536/9 $2.00
doi: 10.1016/j.bpj.2012.04.037

a Lowry assay using BSA as a standard. The molecular weights of the proteins were assumed to be actin, 42,000; myosin S1, 120,000; tropomyosin, 68,000; troponin I, 24,000; troponin T, 35,923; and troponin C, 18,400.

Actin-activated myosin S1 ATPase rates

ATPase rates were measured by the rate of liberation of $^{32}P_i$ from γ^{32}P-ATP (18). Assays were measured at 25°C in reactions containing 0.1 μM S1, 10 μM F-actin, and variable amounts of tropomyosin and troponin in a buffer containing 1 mM ATP, 3 mM $MgCl_2$, 34 mM NaCl, 10 mM MOPS, 1 mM dithiothreitol, 2 mM EGTA, or 0.1 mM $CaCl_2$, pH 7.

ATPase rates were measured as a function of tropomyosin concentrations up to 9.4 μM at an actin concentration of 10 μM. Rates for skeletal S1 decreased from 1.1/s to 0.44/s at tropomyosin concentrations in excess of 0.71 μM (data not shown). A quantity of 2.2 μM tropomyosin was used in most ATPase experiments.

N-ethylmaleimide-treated S1 (NEM-S1) was used to stabilize the active state of regulated actin when ATP was present (19). NEM-S1 was prepared by reacting 4 mg/ml myosin S1 with a 15-fold molar excess of *N*-ethylmaleimide at 25°C for 30 min (20). In ATPase assays, the concentration of regulated actin was increased by an amount equal to the added NEM-S1 concentration to maintain a constant free regulated actin concentration (19).

Fluorescence time courses

Acrylodan-labeled cardiac muscle tropomyosin was prepared as described for skeletal muscle tropomyosin (21) using a 10:1 molar ratio of acrylodan or *N*-(1-pyrene)iodoacetamide to tropomyosin. These conditions gave >70% labeling.

Rapid kinetic measurements were made with a SF20 sequential mixing stopped-flow spectrometer (Applied Photophysics, Leatherhead, UK). A monochromator was used to set the excitation wavelength; the slit width was 0.5 mm. Acrylodan was excited with light at a wavelength of 391 nm and fluorescence was measured through a Schott GG 455 (Duryea, PA) long-pass filter with a 455-nm midpoint or a 450-nm long-pass filter (Edmund Optics, Barrington, NJ). Light-scattering measurements were generally made simultaneously with acrylodan fluorescence measurements using a 425-nm short-pass filter that rejects light between 435 and 635 nm (Edmund Optics).

ATP chase studies

A mixture of 4 μM F-actin, 1.7 μM acrylodan-labeled bovine cardiac tropomyosin, 1.7 μM troponin, and 4 μM myosin S1 were rapidly mixed with a solution containing 4 mM ATP. At these concentrations, the skeletal S1-ATP complex dissociated very rapidly from actin allowing actin-tropomyosin-troponin to return first to the intermediate state (the major state in Ca^{2+}) and then to the inactive state (the major state in EGTA). The transition from the active state to the intermediate state occurred with a decrease in acrylodan fluorescence whereas the subsequent transition to the inactive state occurred with an increase in fluorescence as reported with skeletal tropomyosin-troponin (21). Cardiac S1 was used in some studies, but due to its slower dissociation from actin, the kinetics of thin filament transitions were not readily determined.

The reaction can be described by the scheme shown in Eq. 1 where *M* is myosin, *A* is actin in the active state, and *X* and *I* represent the intermediate and inactive states, respectively:

$$\begin{aligned} &\text{M-A} + \text{ATP} \underset{k_2}{\overset{k_1}{\rightleftharpoons}} \text{ATP-M-A} \underset{k_4}{\overset{k_3}{\rightleftharpoons}} \text{ATP-M} + \text{A} \\ &\text{A} \underset{k_6}{\overset{k_5}{\rightleftharpoons}} \text{X} \underset{k_8}{\overset{k_7}{\rightleftharpoons}} \text{I}. \end{aligned} \tag{1}$$

At high ATP concentrations and with skeletal S1 the values of k_1 and k_2 were sufficiently high that subsequent transitions were unaffected (cardiac S1 produced more complex kinetics). Simulations were done only on rate constants k_3–k_8. The differential equations used to simulate the ATP chase studies were shown earlier (21). S1-ATP detachment was measured by light scattering and was simulated adjusting k_3 so that d[ATP-M-A]/dt matched measured traces. Because the detachment of S1-ATP is virtually complete under the conditions used here, the value of k_4 was set to zero.

Transitions from the active state to the intermediate and inactive states were simulated by varying k_5 and k_7 to match the time courses of A, X, and I to match the observed fluorescence transient. In fitting the data, the observed fluorescence was set equal to

$$F_A * [A] + F_X * [X] + F_I * [I],$$

where F_A, F_X, and F_I are the relative fluorescence intensities of states A, X, and I, respectively. The relative fluorescence of state A, F_A, was set to 1. The value of F_I was 0.95 and F_X was permitted to float in simulations.

Definition of actin states

We previously described the states of regulated actin in the following way: state 1_0 (inactive state with no bound Ca^{2+}), state 1_2 (inactive state with two bound Ca^{2+}), and state 2 (active state) (22). The ATPase activities of myosin S1 in the presence of regulated actin in these states are inactive, intermediate, and active, respectively, and we use those model-independent descriptors of activity here. Another notation is B (blocked) for the state in the absence of Ca^{2+} or bound S1, C (closed or Ca^{2+}) for the major state populated at saturating Ca^{2+}, and M (myosin) for the myosin-activated state. That notation comes from studies of myosin S1 binding to actin in the absence of ATP (23–25) and is not totally appropriate in this case. There is no blocked state in the presence of ATP at ionic strengths ranging from 18 to 134 mM in solution (18,26,27) and up to 170 mM ionic strength in single fibers (28).

RESULTS

We employed ATPase assays and acrylodan tropomyosin fluorescence changes to determine the effect of the Δ14 mutation of TnT on the occupancy of the inactive state of regulated actin. When normalized to the maximum and minimum possible rates, ATPase assays give a functional measure of the occupancy of the active state. Acrylodan tropomyosin fluorescence changes give a measure of the occupancy of the inactive state.

Mutations of troponin may weaken binding to actin-tropomyosin. Fig. 1 shows the dependencies of ATPase rates on the concentrations of troponin (human cardiac TnT and TnC with mouse cardiac TnI) in the absence and presence of Ca^{2+}. In the absence of Ca^{2+}, minimum ATPase activities were reached at ~3 μM troponin in all cases (Fig. 1 *A*). No clear differences were seen in affinity among different troponin types at saturating Ca^{2+}. Concentrations of troponin sufficient to achieve an optimal effect in EGTA were more than adequate to achieve saturation at saturating Ca^{2+}. Note that the S45E TnI mutant produced a level of activity similar to that of actin and tropomyosin alone and no apparent effect of adding troponin was observed at saturating Ca^{2+}.

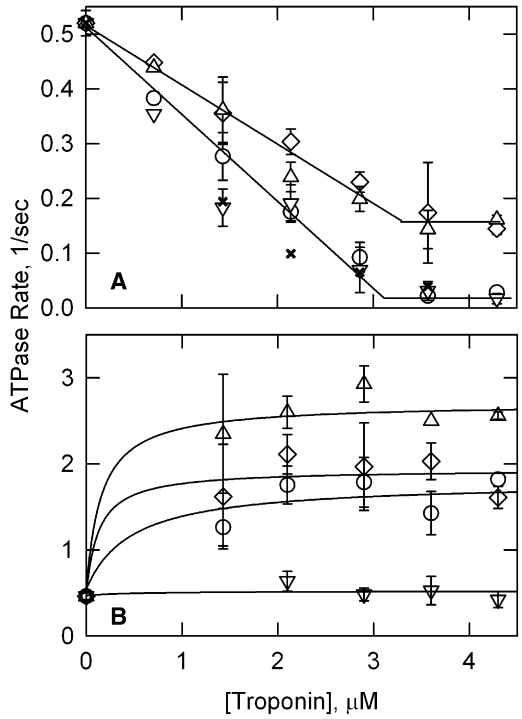

FIGURE 1 Rate of actin-tropomyosin activated myosin S1 ATPase activity as a function of troponin concentration in the absence (*A*) and presence (*B*) of Ca^{2+}. Wild-type cardiac troponin (*circles*), S45E-TnI containing troponin (*inverted triangles*), Δ14 TnT containing troponin (*triangles*), double troponin mutant Δ14 TnT/S45E TnI (*diamonds*), and skeletal troponin (*crosses*). Conditions: 10 μM actin, 2.2 μM tropomyosin, 0.71–4.3 μM troponin (either human cardiac TnT and TnC with mouse cardiac TnI or rabbit skeletal troponin), and 0.1 μM skeletal S1 at 25°C in 34 mM NaCl, 10 mM MOPS, 3 mM $MgCl_2$, 0.1 mM $CaCl_2$ or 2 mM EGTA, 1 mM dithiothreitol, pH 7.

Mutations of troponin affected the ability of regulated actin to stimulate the ATPase activity of skeletal myosin S1. Table 1 summarizes those results. In the absence of Ca^{2+}, the S45E TnI mutant was slightly more inhibitory than wild-type cardiac troponin. Regulated actin filaments containing Δ14 TnT were significantly less inhibitory than the wild-type filaments. Regulated actin filaments containing both S45E TnI and Δ14 TnT (double mutant) were also less inhibitory than wild-type filaments and resembled filaments containing Δ14 TnT alone. Rabbit skeletal troponin, shown as a control, produced a similar degree of inhibition with cardiac tropomyosin as did cardiac troponin but had a greater affinity for the actin-tropomyosin complex.

TABLE 1 Skeletal S1 ATPase rates with wild-type regulated actin and regulated actin containing mutant troponin

	Rate EGTA	Rate Ca^{2+}	NEM-S1 limiting rate	Norm* rate EGTA	Norm* rate Ca^{2+}
Δ14TnT	0.16	2.6	10	0.015	0.29
Δ14TnT/S45E TnI	0.14	1.9	9.2	0.013	0.2
Wild-type	0.028	1.7	9.7	0.0011	0.18
S45E TnI	0.017	0.52	10	0	0.048

10 μM actin, 2.2 μM tropomyosin, ≥ 2.9 μM troponin, 0.1 μM S1 at 25°C in the buffer listed in Fig. 1. The rate of S1 alone was 0.07/s and acto-S1 was 1.1/s.

*Normalized rate = $(v_{obs}-v_{min})/(v_{nem}-v_{min})$. An average value of v_{nem} was used, 9.7/s.

In the presence of saturating Ca^{2+}, regulated actin produced maximum ATPase rates with the order: Δ14 TnT > double mutant > wild-type > S45E TnI. The double mutant had a Ca^{2+}-activated ATPase rate that was between the rates observed for both single mutants. Thus the reduced activation of the S45E TnI mutant compensated for the superior activation of the Δ14 TnT mutant in saturating Ca^{2+}. Competing effects of these mutants did not occur in the absence of Ca^{2+}. The lack of compensation in EGTA indicated that the Δ14 TnT containing actin filaments could not enter the inactive state.

Cardiac S1 ATPase rates were measured with the same hybrid regulated actin filaments. Poor regulation of ATPase activity was obtained unless the S1 was purified as described in Methods. The Δ14 TnT mutant enhanced the regulated actin-activated ATPase activity by 8.2-fold in EGTA (0.14/s vs. 0.017/s) and 2.4-fold in Ca^{2+} (0.60/s vs. 0.25/s). The S45E TnI mutant reduced the activity to 0.53 in EGTA (0.009/s vs. 0.017/s) and 0.68 in Ca^{2+} (0.17/s vs. 0.25/s).

Similar results were obtained with skeletal S1 and troponin containing all human cardiac subunits. In the presence of Ca^{2+}, the ATPase rate with regulated actin containing Δ14 troponin was ~2-fold greater than wild-type (1.6/s vs. 0.83/s). In the absence of Ca^{2+}, the ATPase rate with regulated actin containing Δ14 TnT was ~3-fold of the wild-type value (0.14/s vs. 0.05/s). All ATPase studies suggested that Δ14 TnT stabilized the active state and destabilized the inactive state of regulated actin.

Full stabilization of the active state of regulated actin was achieved by using *N*-ethylmaleimide labeled S1 (NEM-S1). NEM-S1 stabilizes the active state even in the presence of ATP but contributes little to the observed ATP hydrolysis. Fig. 2 shows the NEM-S1 dependencies of skeletal S1 ATPase in the presence of regulated actin having different types of troponin. The solid lines are best fits of a hyperbolic curve to each data set. The rates at high NEM-S1 were relatively independent of mutations in TnT or TnI.

The concentration of NEM-S1 required to give 50% of the limiting ATPase rate increased in order: S45E TnI > wild-type > double mutant > Δ14 TnT (Fig. 2), confirming that Δ14 TnT containing thin filaments were more readily activated than those containing wild-type troponin. This was another indication that the distributions between the intermediate and active states were additive for the two mutants.

The patterns for the ease of activation with NEM-S1 as well as the results of Fig. 1 are consistent with our earlier results (2,3) that Δ14 TnT stabilized the active state and S45E TnI destabilized the active state. This can be seen from the effect of the mutants on the fraction of actin in the active state as given by normalized ATPase rates

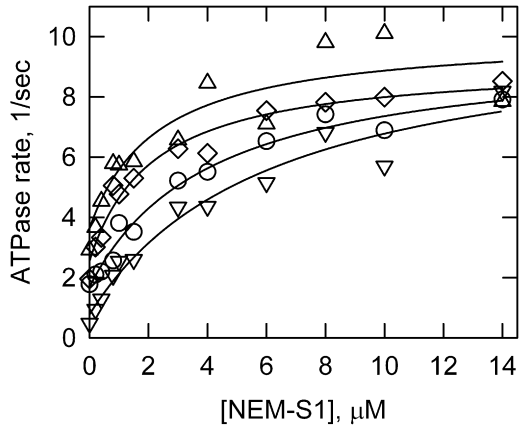

FIGURE 2 NEM-S1 stimulation of actin-tropomyosin-troponin activation of myosin S1 ATPase activities at saturating Ca^{2+}. Wild-type troponin (*circles*), S45E TnI containing troponin (*inverted triangles*), Δ14 TnT containing troponin (*triangles*), double troponin mutant Δ14 TnT/S45E TnI (diamonds). Rates were corrected for contributions from free S1 and NEM-S1. (*Solid lines*) Best fits to each individual curve. The rates at zero NEM-S1 in reciprocal seconds were 0.52 for S45E TnI, 1.7 for wild-type, 1.9 for the double mutant, and 2.6 for Δ14 TnT. The limiting ATPase rates in reciprocal seconds were 0.78 for S45E TnI, 1.7 for wild-type, 2.6 for the double mutant, and 3.6 for Δ14 TnT. The average limiting ATPase rate was 9.7/s. The micromolar concentrations of NEM-S1 required for half-maximum activation were 6, 4, 1.7, and 1.6 for S45E TnI, wild-type, double mutant, and Δ14 TnT, respectively. Initial conditions were the same as in Fig. 1, except 2.9 μM troponin was used and the concentration of regulated actin was raised along with NEM-S1 (see Methods).

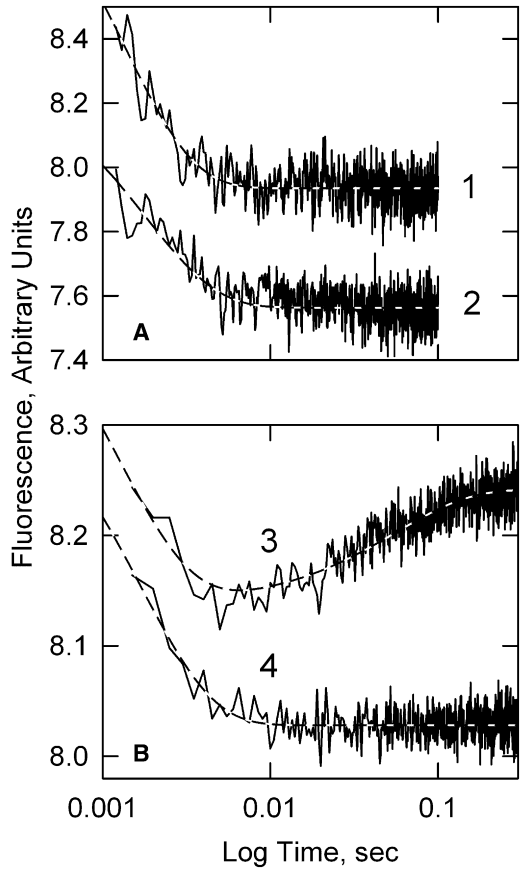

FIGURE 3 Time courses of light scattering (*A*) and acrylodan tropomyosin fluorescence (*B*) changes after rapid S1-ATP detachment from actin-tropomyosin-troponin. (*Curve 1*) Light scattering in EGTA, k_{app} = 700/s. (*Curve 2*) Light scattering in Ca^{2+}, k_{app} = 570/s. (*Curve 3*) Fluorescence in EGTA, k_{app1} = 790/s, k_{app2} = 18/s. (*Curve 4*) Fluorescence in Ca^{2+}, k_{app1} = 670/s. Conditions: 2 μM actin, 0.86 μM tropomyosin, 0.86 μM troponin (human cardiac TnT and TnC with mouse cardiac TnI), 2 μM skeletal S1 in 2 mM ATP, 142 mM KCl, 20 mM MOPS, 6 mM $MgCl_2$, 1 mM dithiothreitol, and either 2 mM EGTA or 0.2 mM $CaCl_2$ at 25°C, pH 7.

(Table 1). The lowest ATPase rate measured was that with regulated actin containing S45E TnI in EGTA; that rate was set equal to zero. The limiting rate at high NEM-S1 was set to 1.

The failure of the S45E TnI mutant to rescue the Δ14 TnT mutant in the absence of Ca^{2+} could be explained by an inability of Δ14 TnT containing regulated actin to form the inactive state. The transition to the inactive state can be measured directly using an acrylodan probe on tropomyosin (21).

Fig. 3 *A* shows time courses of S1-ATP detachment from actin-tropomyosin-troponin as measured by light scattering. Ca^{2+} had little effect on the rate constant for skeletal S1-ATP detachment. Fig. 3 *B* shows changes in fluorescence emission intensity from acrylodan-tropomyosin that were measured simultaneously with the light-scattering changes. Acrylodan-tropomyosin fluorescence decreased rapidly, in the presence of Ca^{2+}, with a rate constant that was similar to that of the light-scattering transition. The rapid decrease in fluorescence represented the change from the active state to an equilibrium mixture of states dominated by the intermediate state. Therefore, the rate of transition of tropomyosin to the intermediate state was greater or equal to the rate of dissociation of S1-ATP from regulated actin.

In the absence of Ca^{2+}, the rapid fluorescence decrease was followed by a slower fluorescence increase as regulated actin moved to the inactive state (Fig. 3 *B*).

Conditions for measuring the transition from the active state to the intermediate and inactive states were optimized by varying concentrations of troponin, S1, and ATP. The initial rapid decrease in acrylodan fluorescence was insensitive to the troponin concentration. Increasing troponin from 0.43 to 0.86 μM produced a change in the slower fluorescence increase from a biexponential to a monoexponential signal (data not shown). At low troponin concentrations the slow fluorescence increase was preceded by a more rapid increase. We used the presence of a monoexponential increase as evidence of troponin saturation.

The largest amplitudes for the fluorescence transitions occurred when the ratio of bound S1 to actin was 1:1. The amplitude of the signal approached zero as the S1 concentration approached zero. No changes in kinetics were observed among traces of different S1 concentrations where a signal was observed (data not shown).

Transients of acrylodan tropomyosin fluorescence, after dissociation of skeletal S1-ATP, changed qualitatively as the ATP concentration was decreased (Fig. 4 *A*). The fluorescence redevelopment characteristic of entering the inactive state was not seen at 0.05 mM ATP. The transition to the inactive state was first observed at 0.1 mM ATP but the observed rate was very slow and limited by the slow rate of S1-ATP detachment. Accurate measurement of the kinetics of transition to the inactive state required rapid ATP binding and rapid detachment of S1-ATP.

Fig. 4 *B* shows a plot of apparent rate constants for the transition to the intermediate and inactive states at ≈11°C at varied concentrations of ATP. Fig. 4 *C* shows the same at ≈2°C. Measurements of the apparent rate constant for formation of the inactive state were approximately constant above 0.5 mM ATP at both temperatures.

Similar studies were done with cardiac S1 but the resulting kinetics were complicated by a population of slowly detaching cardiac S1. The population of slowly detaching S1 was reduced, but not eliminated, by removing ATP resistant S1 as described in Methods. Fig. 4 *D* shows that after dissociation of cardiac S1-ATP there was a rapid decrease in fluorescence followed by a slower fluorescence recovery that occurred only when ATP was in excess of 0.1 mM. The slow fluorescence increase had a smaller amplitude with cardiac S1 than observed with skeletal S1. Simulations of the data indicated that the reduced amplitude resulted from slower cardiac S1 detachment rates.

Fig. 4 *E* shows the rate of light-scattering decrease after rapid addition of ATP to the complex of cardiac S1 bound to regulated actin. The dissociation of purified cardiac S1 from regulated actin was biexponential. The apparent rate constants for each process are shown together with the fraction of the light scattering signal due to the fast process (*inset*). Although the rate of the fast process was near 600/s at high ATP concentrations, the slow phase did not exceed 40/s. At 10 mM ATP, the slow phase accounted for 20% of the total signal and limited the kinetics of the subsequent transitions of regulated actin.

Fig. 4 *F* shows the ATP dependence of the apparent rate constants for actin transitions measured by the dissociation

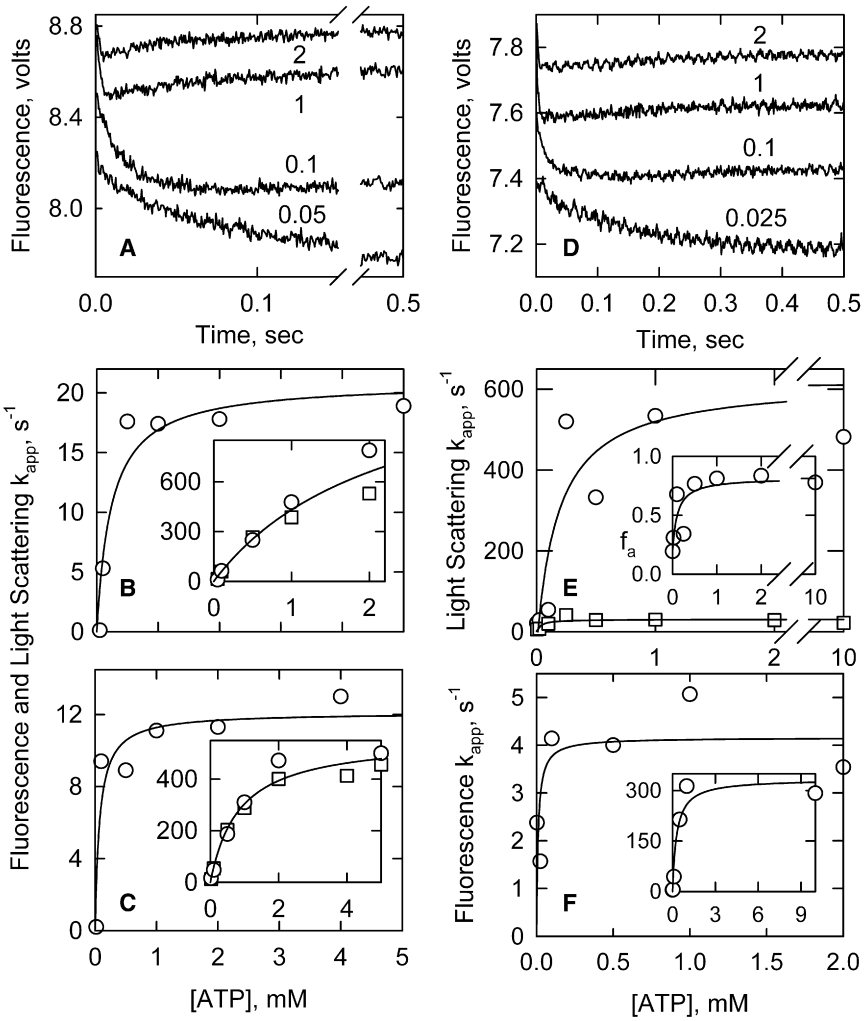

FIGURE 4 ATP dependence of the kinetics of acrylodan fluorescence changes during transition from the active state to the inactive state of actin-tropomyosin-troponin. Panels *A–C* are experiments with skeletal S1. (*A*) Time courses at 11°C for acrylodan tropomyosin fluorescence changes at various [ATP] given as mM in the figure. (*B* and *C*) Apparent rate constants for the transitions to the inactive state and to the intermediate state (*inset*) at varied [ATP] at 11°C (*B*) and 2°C (*C*). (*Open circles*) Apparent rate constants for the acrylodan tropomyosin fluorescence transitions; (*squares*) apparent rate constants for light-scattering transitions. (*D–F*) Experiments with cardiac S1. (*D*) Time courses at 7°C for acrylodan tropomyosin fluorescence changes at [ATP] given in the figure as mM. (*E*) Fast (*circles*) and slow (*squares*) phases of cardiac S1-ATP dissociation from regulated actin. (*Inset*) f_a (fraction of total amplitude contributed by the fast component) vs. [ATP]. (*F*) Apparent rate constants for the acrylodan-tropomyosin fluorescence transitions for the slow phase and fast phase (*inset*). Conditions: 2 μM actin, 0.86 μM acrylodan-tropomyosin, 0.86 μM troponin (human cardiac TnT and TnC with mouse cardiac TnI), and 2 μM S1 in the same buffer as in Fig. 3.

of cardiac S1. The apparent rate constants of both the fast and slow processes were reduced compared with those measured with skeletal S1 (Fig. 4 *C*) as a result of reduced cardiac S1 detachment kinetics. Skeletal S1 was used in subsequent studies because of its more rapid detachment kinetics.

Fig. 5 compares the acrylodan tropomyosin transients of regulated actin containing various types of troponin. In all cases, the presence of Δ14 TnT virtually eliminated the slow fluorescence change associated with transition to the inactive state. Fig. 5 *A* shows acrylodan tropomyosin fluorescence transients in EGTA for studies with skeletal S1, human cardiac TnT and TnC, and mouse cardiac TnI. Regulated actin containing either wild-type troponin or troponin containing S45E TnI exhibited the fluorescence increase indicative of formation of the inactive state. Regulated actin containing Δ14 TnT did not exhibit the slow fluorescence increase. The presence of the S45E TnI mutant did not rescue the fluorescence increase in the presence of Δ14 TnT. These observations were made at 2°, 7°, 11°, 15°, and 20°C, but only those at 11°C are shown.

Fig. 5 *B* shows the transition among the states of regulated actin for studies done with skeletal S1 and human cardiac TnI. Fig. 5 *C* shows similar studies with cardiac S1 and human cardiac TnI. In both cases, regulated actin containing wild-type troponin exhibited a rapid fluorescence decrease followed by a slower increase showing a robust transition to the inactive state. When the 14 C-terminal residues of TnT were absent, the signal was attenuated and little, if any, transition to the inactive state occurred.

DISCUSSION

The key observation in this report is that deletion of the 14 C-terminal residues of cardiac TnT greatly reduced or eliminated the occupancy of the inactive or blocked state. This conclusion was based on enhanced activation of ATPase activity in the absence and presence of calcium and changes in acrylodan-tropomyosin fluorescence.

Upon dissociating S1-ATP from regulated actin filaments containing acrylodan-labeled tropomyosin there is a rapid decrease in fluorescence followed by a slower fluorescence increase (21). The initial fluorescence phase is due to a transition from the active state to the intermediate state whereas the second phase monitors the transition to the inactive state. In the case of Δ14 TnT-containing regulated actin, there was little or no evidence of the second phase even in the presence of S45E TnI that favors the inactive state.

Measurements of the fluorescence transitions require that the binding of ATP to S1 and the subsequent dissociation of S1 from regulated actin be rapid compared to the two subsequent fluorescence transitions. Skeletal S1 dissociates rapidly. The kinetics and amplitude of the transition from the intermediate state to the inactive state are reliable, although the rate constant for the transition from the active

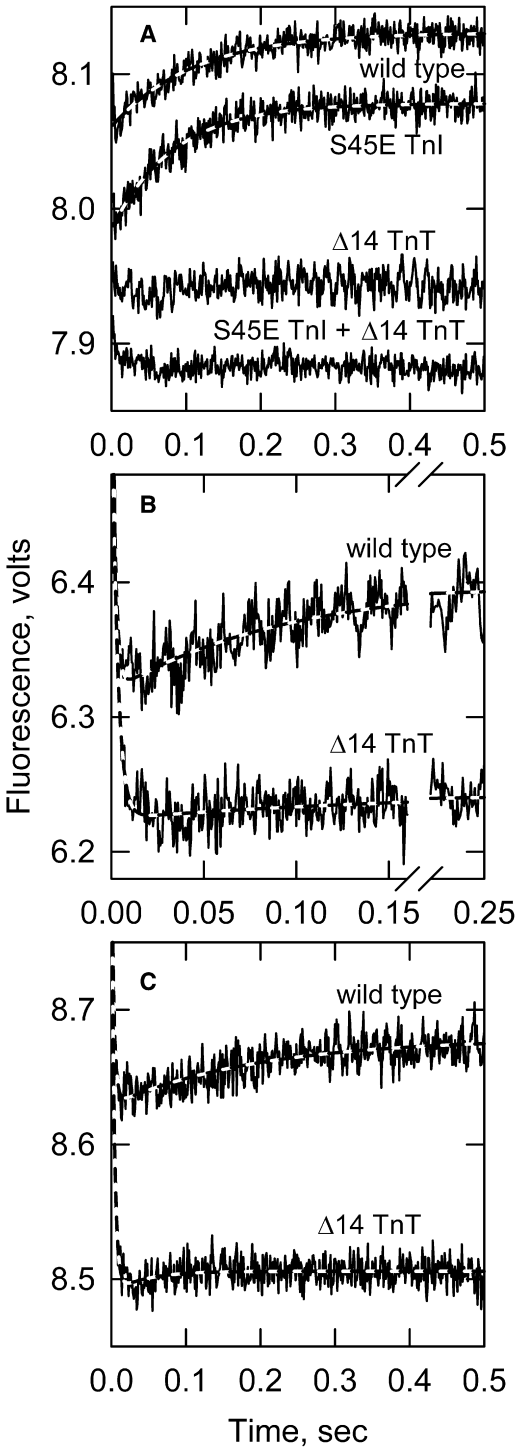

FIGURE 5 Transition of actin-tropomyosin-troponin from the active state to the intermediate and inactive states after rapid dissociation of S1-ATP. (*A*) Measurements with skeletal S1, human cardiac TnT, and TnC and mouse cardiac TnI at 11°C. k_{app} (slow phase) = 9.1/s for wild-type and 12.0/s for S45E. (*B*) Measurements with skeletal S1 and human cardiac troponin subunits at 7°C. k_{app} (slow phase) = 10.5/s for wild-type. (*C*) Measurements with cardiac S1 and human cardiac troponin subunits at 7°C. k_{app} (slow phase) = 5.1/s for wild-type. Conditions: 2 μM actin, 0.86 μM acrylodan-tropomyosin, 0.86 μM troponin, 2 μM S1, and 2 mM ATP in the same buffer as in Fig. 3.

state to the intermediate state could be underestimated. Cardiac S1-ATP dissociation, on the other hand, had a slow phase that interfered with measurement of both fluorescence transitions. That slow phase may have resulted from β-cardiac S1 that has a 5–10-fold higher affinity for actin than the α-isoform (29).

Simulations of the transitions indicated that, as the rate constant for S1-ATP release decreased below 200/s, the second fluorescence transient became smaller. When the rate constant for S1-ATP release reached 50/s the second transient was 50% of its true value. The apparent rate constant for the second phase of cardiac S1 dissociation was 30/s. Therefore, measurements made with skeletal S1 are more reliable.

The C-terminal 14 residues of TnT appear to be essential for stabilizing the inactive state and/or for generating the signal indicative of the inactive state or both. The acrylodan probe is present at Cys-190 of tropomyosin. There is evidence that the C-terminal region of TnT binds near that region (30) but is disrupted when Ca^{2+} is bound to the regulatory lobe of troponin C (31).

There is evidence that the region of TnT that binds near Cys-190 is within the C-terminal 31 (31) or 17 residues (32) of troponin T. If true, then the slower increase in acrylodan fluorescence that we observe could be due to binding of the C-terminal region of TnT to area near the acrylodan probe. However, another study localized the TnT2 tropomyosin-binding region to a 25-amino-acid segment of TnT near the beginning of the TnT2 region (between residues 197 and 239 for human cTnT) (33).

Evidence that the slower increase in acrylodan fluorescence is indicative of formation of the inactive/blocked state comes from past (21) and present correlations of the fluorescence changes with ATPase activity. Regulated actin can be trapped in the active/M state in the absence of Ca^{2+} by rigor S1 binding. After rapid S1-ATP dissociation, the regulated actin returns to its most stable state—the inactive/blocked state. This occurs with a rapid decrease in fluorescence followed by a slower fluorescence increase. That slower increase occurs only in the absence of Ca^{2+} where the inactive state forms (21). We saw that, when the C-terminal 14 residues of TnT are absent, the slow fluorescence increase did not occur.

We also observed, with highly reproducible skeletal S1 ATPase activities, that actin filaments containing Δ14 TnT had an ATPase rate greater than wild-type actin filaments in the absence of Ca^{2+}. Those ATPase rates indicated that actin filaments containing Δ14 TnT were not in the fully inactive state. Rather, the results are consistent with the Δ14 TnT-regulated actin existing in the intermediate/closed state in the absence of Ca^{2+}.

Table 1 shows that in EGTA, regulated actin containing Δ14 TnT has ~1.5% of the ability to stimulate ATP hydrolysis as filaments in the fully active state. That agrees with estimates of the relative activating ability of the intermediate state determined from an analysis of the properties of R146G and R146W mutants of TnI that stabilize the intermediate state (1). The earlier estimate placed the ratio of activity of the intermediate state to the NEM-S1 activated rate to be between 0.04 and 0.15. That corresponds to normalized rates between 1.4 and 2.2% using the method of calculation given in Table 1.

The low ability of the intermediate state of regulated actin to stimulate myosin ATPase activity means that there are two inactive states. Multiple inactive states may act as a reservoir to lower the population of the active state. The transition from the inactive state to the intermediate state is sensitive to Ca^{2+} and to high affinity S1 (i.e., S1-ADP) binding whereas the transition of the intermediate state to the active state is sensitive only to high affinity S1 binding (i.e., S1-ADP). This arrangement gives multiple control points and may be involved in phosphorylation-dependent modulation of cardiac regulation (34).

The experimental difficulty with multiple inactive states is that it can be difficult to determine which state is occupied in a particular situation. By normalizing the activities as in Table 1 it is possible to detect small changes in activity. Changes in acrylodan-tropomyosin fluorescence as shown in Figs. 3–5 present a convenient signature for detecting changes in the inactive state.

Our results are consistent with earlier measurements made with C-terminal truncation mutants of TnT. When examined in rabbit psoas fibers, Δ14 TnT did not significantly affect force, but increased Ca^{2+} sensitivity (3). Increased Ca^{2+} sensitivity was also observed for another TnT truncation mutant, Δ28+7 (35,36). The increased Ca^{2+} sensitivity is consistent with destabilization of the inactive state and stabilization of the active state. In transgenic mice, the Δ28+7 TnT mutation resulted in impaired diastolic and systolic function (37). The inability to relax completely may be due in part to loss of the inactive/blocked state. Reduced inhibition of in vitro motility was observed for actin filaments containing Δ28+7 TnT (38). This is another example where modifications of the C-terminal region of TnT prevent full relaxation.

A possible scenario for the interactions that stabilize the inactive state is shown in Fig. 6. Binding of the inhibitory region of TnI to actin is thought to be essential for holding tropomyosin in the inactive state (39–42). The C-terminal region of TnI (C-TnI) also binds to the interhelical region of actin in the inhibited state (43). We show here that the C-terminus of TnT (C-TnT) or specifically the region SKTRGKAKVTGRWK is also required to have a stable inactive state. This region is within the C-terminal 17-amino-acid region that is unstructured (42). Based on evidence given earlier in this discussion, that C-terminal region of TnT may bind to tropomyosin near Cys-190 within period 5. The inhibitory and switch regions of TnI (40,41) are also near the period-5 region of tropomyosin (44) when regulated actin is in the inactive state.

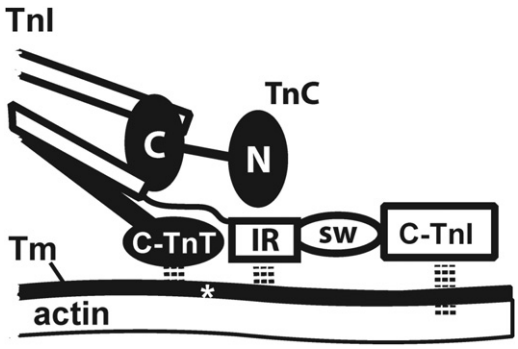

FIGURE 6 Schematic of possible interactions of TnI and TnT with actin-tropomyosin in the relaxed state. The scheme is based on the published crystal structure of the core region of troponin (42). Only that portion of the regulatory complex containing the interaction sites is shown. TnC is shown as a dumbbell. (*Bold lines*)Two of the TnI helices and the inhibitory region (IR), the switch region (SW), and the C-terminal region between residues 164 and 210 (C-TnI) are shown. (*Black*) TnT helix and the C-terminal region encompassing residues 271–288 (C-TnT). (*Parallel dotted lines*) Putative interactions with actin and tropomyosin in the absence of Ca^{2+}. (*Asterisk*) Cys-190 of tropomyosin.

The authors thank Dr. David M. Warshaw for sharing his procedure for removing ATP-resistant S1, and Dr. Howard D. White and Ms. Betty Belknap for sharing their procedure for making cardiac S1.

This work was funded by grant No. AR035216 from the National Institutes of Health to J.M.C. and grant No. R01HL082923 to T.K.

REFERENCES

1. Mathur, M. C., T. Kobayashi, and J. M. Chalovich. 2009. Some cardiomyopathy-causing troponin I mutations stabilize a functional intermediate actin state. *Biophys. J.* 96:2237–2244.
2. Mathur, M. C., T. Kobayashi, and J. M. Chalovich. 2008. Negative charges at protein kinase C sites of troponin I stabilize the inactive state of actin. *Biophys. J.* 94:542–549.
3. Gafurov, B., S. Fredricksen, …, J. M. Chalovich. 2004. The Delta 14 mutation of human cardiac troponin T enhances ATPase activity and alters the cooperative binding of S1-ADP to regulated actin. *Biochemistry.* 43:15276–15285.
4. Varughese, J. F., J. M. Chalovich, and Y. Li. 2010. Molecular dynamics studies on troponin (TnI-TnT-TnC) complexes: insight into the regulation of muscle contraction. *J. Biomol. Struct. Dyn.* 28:159–174.
5. Bremel, R. D., J. M. Murray, and A. Weber. 1972. Manifestations of cooperative behavior in the regulated actin filament during actin-activated ATP hydrolysis in the presence of calcium. *Cold Spring Harb. Symp. Quant. Biol.* 37:267–275.
6. Greene, L. E., and E. Eisenberg. 1980. Cooperative binding of myosin subfragment-1 to the actin-troponin-tropomyosin complex. *Proc. Natl. Acad. Sci. USA.* 77:2616–2620.
7. Tardiff, J. C. 2011. Thin filament mutations: developing an integrative approach to a complex disorder. *Circ. Res.* 108:765–782.
8. Spudich, J. A., and S. Watt. 1971. The regulation of rabbit skeletal muscle contraction. I. Biochemical studies of the interaction of the tropomyosin-troponin complex with actin and the proteolytic fragments of myosin. *J. Biol. Chem.* 246:4866–4871.
9. Eisenberg, E., and W. W. Kielley. 1974. Troponin-tropomyosin complex. Column chromatographic separation and activity of the three, active troponin components with and without tropomyosin present. *J. Biol. Chem.* 249:4742–4748.
10. Kielley, W. W., and W. F. Harrington. 1960. A model for the myosin molecule. *Biochim. Biophys. Acta.* 41:401–421.
11. Siemankowski, R. F., and P. Dreizen. 1978. Canine cardiac myosin with special reference to pressure overload cardiac hypertrophy. I. Subunit composition. *J. Biol. Chem.* 253:8648–8658.
12. Siemankowski, R. F., and H. D. White. 1984. Kinetics of the interaction between actin, ADP, and cardiac myosin-S1. *J. Biol. Chem.* 259:5045–5053.
13. Weeds, A. G., and R. S. Taylor. 1975. Separation of subfragment-1 isoenzymes from rabbit skeletal muscle myosin. *Nature.* 257:54–56.
14. Lauzon, A. M., M. J. Tyska, …, K. M. Trybus. 1998. A 7-amino-acid insert in the heavy chain nucleotide binding loop alters the kinetics of smooth muscle myosin in the laser trap. *J. Muscle Res. Cell Motil.* 19:825–837.
15. Smillie, L. B. 1982. Preparation and identification of α- and β-tropomyosins. *In* Methods in Enzymology, *85*. Academic Press, New York. 234–241.
16. Potter, J. D. 1982. Preparation of troponin and its subunits. *In* Methods in Enzymology, *85*. Academic Press, New York. 241–263.
17. Kobayashi, T., and R. J. Solaro. 2006. Increased Ca^{2+} affinity of cardiac thin filaments reconstituted with cardiomyopathy-related mutant cardiac troponin I. *J. Biol. Chem.* 281:13471–13477.
18. Chalovich, J. M., and E. Eisenberg. 1982. Inhibition of actomyosin ATPase activity by troponin-tropomyosin without blocking the binding of myosin to actin. *J. Biol. Chem.* 257:2432–2437.
19. Williams, Jr., D. L., L. E. Greene, and E. Eisenberg. 1988. Cooperative turning on of myosin subfragment 1 adenosinetriphosphatase activity by the troponin-tropomyosin-actin complex. *Biochemistry.* 27:6987–6993.
20. Chalovich, J. M., E. Lutz, …, M. M. Schroeter. 2011. Acrylodan-labeled smooth muscle tropomyosin reports differences in the effects of troponin and caldesmon in the transition from the active state to the inactive state. *Biochemistry.* 50:6093–6101.
21. Borrego-Diaz, E., and J. M. Chalovich. 2010. Kinetics of regulated actin transitions measured by probes on tropomyosin. *Biophys. J.* 98: 2601–2609.
22. Hill, T. L., E. Eisenberg, and J. M. Chalovich. 1981. Theoretical models for cooperative steady-state ATPase activity of myosin subfragment-1 on regulated actin. *Biophys. J.* 35:99–112.
23. McKillop, D. F. A., and M. A. Geeves. 1993. Regulation of the interaction between actin and myosin subfragment 1: evidence for three states of the thin filament. *Biophys. J.* 65:693–701.
24. Trybus, K. M., and E. W. Taylor. 1980. Kinetic studies of the cooperative binding of subfragment 1 to regulated actin. *Proc. Natl. Acad. Sci. USA.* 77:7209–7213.
25. Shitaka, Y., C. Kimura, and M. Miki. 2005. The rates of switching movement of troponin T between three states of skeletal muscle thin filaments determined by fluorescence resonance energy transfer. *J. Biol. Chem.* 280:2613–2619.
26. Resetar, A. M., J. M. Stephens, and J. M. Chalovich. 2002. Troponin-tropomyosin: an allosteric switch or a steric blocker? *Biophys. J.* 83:1039–1049.
27. el-Saleh, S. C., and J. D. Potter. 1985. Calcium-insensitive binding of heavy meromyosin to regulated actin at physiological ionic strength. *J. Biol. Chem.* 260:14775–14779.
28. Kraft, T., J. M. Chalovich, …, B. Brenner. 1995. Parallel inhibition of active force and relaxed fiber stiffness by caldesmon fragments at physiological ionic strength and temperature conditions: additional evidence that weak cross-bridge binding to actin is an essential intermediate for force generation. *Biophys. J.* 68:2404–2418.
29. Deacon, J. C., M. J. Bloemink, …, L. A. Leinwand. 2012. Identification of functional differences between recombinant human α and β cardiac myosin motors. *Cell. Mol. Life Sci.* 10.1007/s00018-012-0927-3.
30. Morris, E. P., and S. S. Lehrer. 1984. Troponin-tropomyosin interactions. Fluorescence studies of the binding of troponin, troponin T,

and chymotryptic troponin T fragments to specifically labeled tropomyosin. *Biochemistry.* 23:2214–2220.

31. Pearlstone, J. R., and L. B. Smillie. 1981. Identification of a second binding region on rabbit skeletal troponin-T for α-tropomyosin. *FEBS Lett.* 128:119–122.
32. Tanokura, M., Y. Tawada, …, I. Ohtsuki. 1983. Chymotryptic subfragments of troponin T from rabbit skeletal muscle. Interaction with tropomyosin, troponin I and troponin C. *J. Biochem.* 93:331–337.
33. Jin, J. P., and S. M. Chong. 2010. Localization of the two tropomyosin-binding sites of troponin T. *Arch. Biochem. Biophys.* 500:144–150.
34. Solaro, R. J., and T. Kobayashi. 2011. Protein phosphorylation and signal transduction in cardiac thin filaments. *J. Biol. Chem.* 286: 9935–9940.
35. Montgomery, D. E., J. C. Tardiff, and M. Chandra. 2001. Cardiac troponin T mutations: correlation between the type of mutation and the nature of myofilament dysfunction in transgenic mice. *J. Physiol.* 536:583–592.
36. Stelzer, J. E., J. R. Patel, …, R. L. Moss. 2004. Expression of cardiac troponin T with COOH-terminal truncation accelerates cross-bridge interaction kinetics in mouse myocardium. *Am. J. Physiol. Heart Circ. Physiol.* 287:H1756–H1761.
37. Tardiff, J. C., S. M. Factor, …, L. A. Leinwand. 1998. A truncated cardiac troponin T molecule in transgenic mice suggests multiple cellular mechanisms for familial hypertrophic cardiomyopathy. *J. Clin. Invest.* 101:2800–2811.
38. Redwood, C., K. Lohmann, …, H. Watkins. 2000. Investigation of a truncated cardiac troponin T that causes familial hypertrophic cardiomyopathy: Ca^{2+} regulatory properties of reconstituted thin filaments depend on the ratio of mutant to wild-type protein. *Circ. Res.* 86: 1146–1152.
39. Li, M. X., X. Wang, and B. D. Sykes. 2004. Structural based insights into the role of troponin in cardiac muscle pathophysiology. *J. Muscle Res. Cell Motil.* 25:559–579.
40. Malnic, B., C. S. Farah, and F. C. Reinach. 1998. Regulatory properties of the NH2- and COOH-terminal domains of troponin T. ATPase activation and binding to troponin I and troponin C. *J. Biol. Chem.* 273: 10594–10601.
41. Murakami, K., F. Yumoto, …, T. Wakabayashi. 2005. Structural basis for Ca^{2+}-regulated muscle relaxation at interaction sites of troponin with actin and tropomyosin. *J. Mol. Biol.* 352:178–201.
42. Takeda, S., A. Yamashita, …, Y. Maéda. 2003. Structure of the core domain of human cardiac troponin in the Ca^{2+}-saturated form. *Nature.* 424:35–41.
43. Murakami, K., F. Yumoto, …, T. Wakabayashi. 2007. Structural basis for calcium-regulated relaxation of striated muscles at interaction sites of troponin with actin and tropomyosin. *Adv. Exp. Med. Biol.* 592: 71–86.
44. Oguchi, Y., J. Ishizuka, …, M. Kawai. 2011. The role of tropomyosin domains in cooperative activation of the actin-myosin interaction. *J. Mol. Biol.* 414:667–680.